3-1-2009

The Effect of Silicon Content on Impact Toughness of T91 Grade Steels

Ajit K. Roy
University of Nevada, Las Vegas, aroy@unlv.nevada.edu

Pankaj Kumar
University of Nevada, Las Vegas

Debajyoti Maitra
University of Nevada, Las Vegas

JMEPEG (2009) 18:205–210
DOI: 10.1007/s11665-008-9271-z

1059-9495/$19.00

The Effect of Silicon Content on Impact Toughness of T91 Grade Steels

Ajit Roy, Pankaj Kumar, and Debajyoti Maitra

(Submitted March 7, 2008; in revised form May 20, 2008)

The impact resistance of silicon (Si)-containing modified 9Cr-1Mo steels has been investigated within a temperature regime of −40 to 440 °C using the Charpy method. The results indicate that the energies absorbed in fracturing the tested specimens were substantially lower at temperatures of −40, 25, and 75 °C compared to those at elevated temperatures. Lower impact energies and higher ductile-to-brittle-transition-temperatures (DBTTs) were observed with the steels containing 1.5 and 1.9 wt.% Si. The steels containing higher Si levels exhibited both ductile and brittle failures at elevated temperatures. However, at lower temperatures, brittle failures characterized by cleavage and intergranular cracking were observed for all four tested materials.

Keywords DBTT, fractography, impact energy, silicon effect, T91 grade steels

1. Introduction

Transmutation of spent nuclear fuels (SNF) is currently being considered to enable their efficient disposal for shorter duration at the proposed yucca mountain geologic repository, located in Nevada. The process of transmutation involves transformation of highly radioactive SNF to species with shorter half-lives by changes in the nucleus of radioactive elements resulting from natural radioactive decay, nuclear fission, neutron capture, and other related processes. This process is expected to generate and subsequently separate minor actinides and fission products by impinging proton-generated neutrons onto SNF at a very high speed (Ref 1). Target materials such as tungsten and molten lead-bismuth-eutectic (LBE) have been extensively used to generate neutrons by bombarding accelerator-driven protons onto them. The target material has to be contained inside a structural vessel made of a suitable metal or an alloy. Martensitic iron-chromium-molybdenum (Fe-Cr-Mo) alloys such as modified 9Cr-1Mo steels have been identified (Ref 2-5) to be the suitable structural materials to contain the target material.

Studies performed (Ref 6, 7) at the author's laboratories have exhibited a beneficial effect of silicon (~1.0 wt.%) on both the corrosion and tensile properties of Fe-Cr-Mo alloys. These materials may be subjected to impact loading during the neutron generation process, known as spallation. In view of these rationales, the effect of silicon (Si) content on the impact resistance of modified 9Cr-1Mo steels, also known as T91 grade steels, has been investigated. This article presents the results of impact testing of T91 grade steels as a function of Si content so that an optimum Si content could be identified to provide the desired toughness in terms of impact energy and ductile-to-brittle transition temperature (DBTT). The resultant data using Charpy v-notch (CVN) specimens have also been substantiated using fractographic evaluations performed by scanning electron microscopy.

2. Materials and Experimental Procedure

Experimental heats (100 lbs each) of martensitic T91 grade steels containing four levels of Si (0.5, 1.0, 1.5, and 1.9 wt.%) were custom-melted at a vendor's facility using a vacuum induction melting practice. These heats were subsequently processed into rectangular bars of desired dimensions by forging and hot-rolling. The hot-rolled bars were subjected to thermal treatment that consisted of austenitizing at 1110 °C (1850 °F) for 1 h and oil quenching. The quenched materials were subsequently tempered at 621 °C (1150 °F) for 1 h followed by air-cooling. A combination of quenching and tempering was aimed at producing fully tempered and fine-grained martensitic microstructure throughout the matrix of the test materials without the formation of retained austenite. The chemical compositions of all four heats of materials are given in Table 1.

The tensile properties of all four heats of T91 grade steels were determined using smooth cylindrical specimens according to the ASTM Designation E 8 (Ref 8). These specimens had a 101.4-mm (4 in.) overall length, a gage length of 25.4-mm (1 in.), and a gage diameter of 6.35-mm (0.25 in.). CVN specimens having 54.96-mm (2.16 in.) length, 10-mm (0.39 in.) width, 8-mm (0.32 in.) thickness, and a notch angle of 45° were machined from the heat-treated materials in such a way that the plane containing the notch was parallel to the longitudinal rolling direction. A pictorial view of the CVN specimen, machined according to the ASTM Designation E 23

Ajit Roy, Pankaj Kumar, and **Debajyoti Maitra**, Department of Mechanical Engineering, University of Nevada, Las Vegas (UNLV), 4505 Maryland Parkway, Box 454027, Las Vegas, NV 89154-4027. Contact e-mail: aroy@unlv.nevada.edu.

Table 1 Chemical composition of T91 grade steels

	Elements, wt.%											
Heat no.	**C**	**Mn**	**P**	**S**	**Si**	**Ni**	**Cr**	**Mo**	**Al**	**V**	**Cb**	**N, ppm**	**Fe**
2403	.12	.44	.004	.003	.48	.30	9.38	1.03	.024	.23	.91	57	Bal
2404	.12	.45	.004	.003	1.02	.30	9.61	1.03	.025	.24	.89	53	Bal
2405	.11	.45	.004	.004	1.55	.31	9.66	1.02	.024	.24	.085	49	Bal
2406	.11	.45	.004	.004	1.88	.31	9.57	1.01	.029	.24	.087	30	Bal

Note: Bal, balance

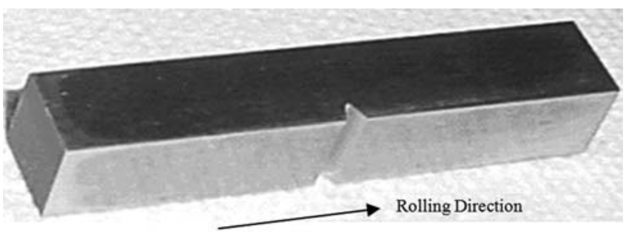

Fig. 1 Pictorial view of CVN specimen

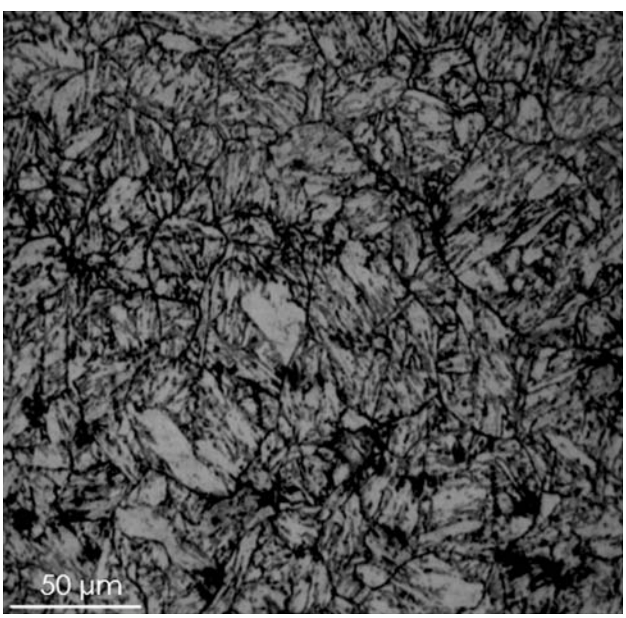

Fig. 2 Optical micrograph of steel with 0.5 wt.% Si, Beraha's reagent

(Ref 9), is illustrated in Fig. 1. A commercially available pendulum-type impact tester was used to strike the CVN specimens at a location opposite to the notch. A dial indicator attached to this equipment recorded the energy absorbed to fracture the specimens in terms of either Joules or feet-pounds (ft-lbs). The CVN specimens were tested at temperatures ranging from cryogenic (−40 °C) to 440 °C. A maximum temperature of 440 °C was used to simulate the operating temperature used in the spallation process involving molten LBE as a target and a coolant. The cryogenic temperature was attained by immersing these specimens inside an insulated

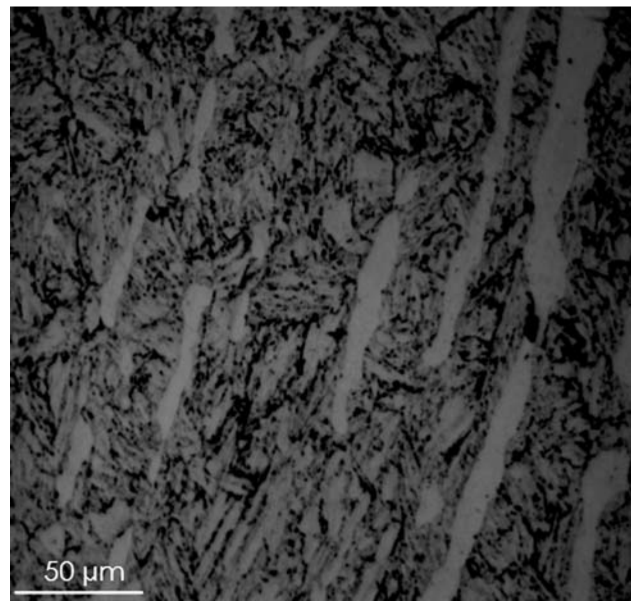

Fig. 3 Optical micrograph of steel with 1.0 wt.% Si, Beraha's reagent

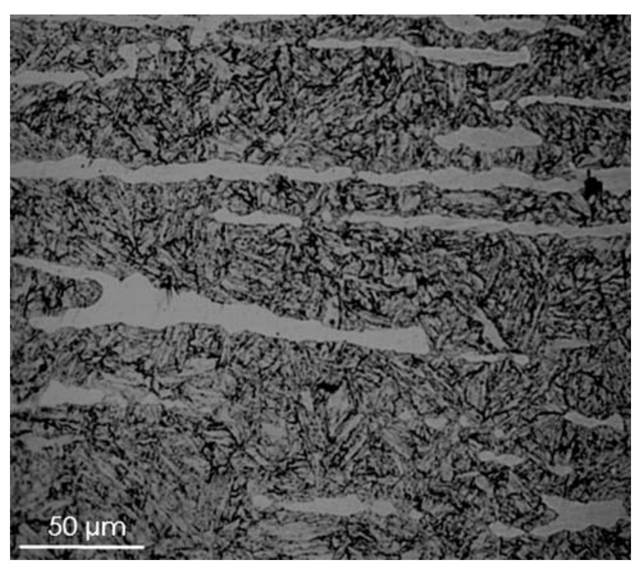

Fig. 4 Optical micrograph of steel with 1.5 wt.% Si, Beraha's reagent

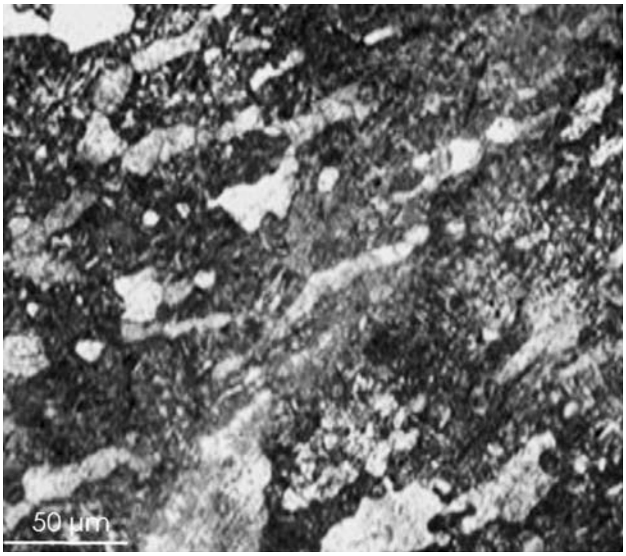

Fig. 5 Optical micrograph of steel with 1.9 wt.% Si, Beraha's reagent

Table 2 Room temperature tensile properties of T91 grade steels

Heat no. (Si content)	UTS, MPa	YS, MPa	%El	%RA
2403 (0.5%)	1014	876	23	67.4
2404 (1.0%)	986	862	21	65.7
2405 (1.5%)	1020	904	24	68.1
2406 (1.9%)	1027	903	26	76.2

Table 3 Results of charpy testing

Si content, wt.%	Temperature, °C Impact energy, ft-lb −40	25	75	125	230	340	440	DBTT, °C
0.5	15	19	27	48	59	62	63	90
1.0	8.5	13	18	38	47.5	49	49	95
1.5	4.5	8	12.5	19	31	38	39	140
1.9	3	6	8	13	23	28	30.5	150

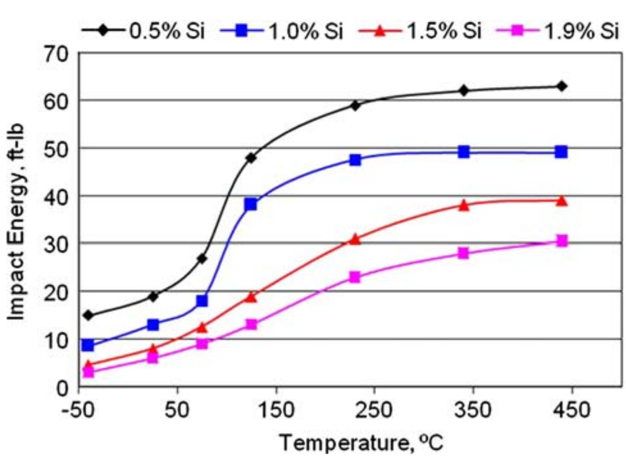

Fig. 6 Variation of impact energy with temperature

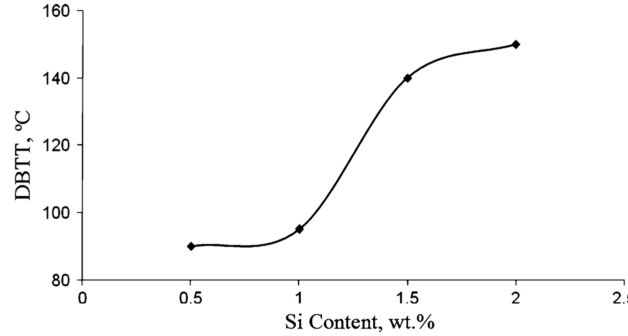

Fig. 7 Variation of DBTT with Si content

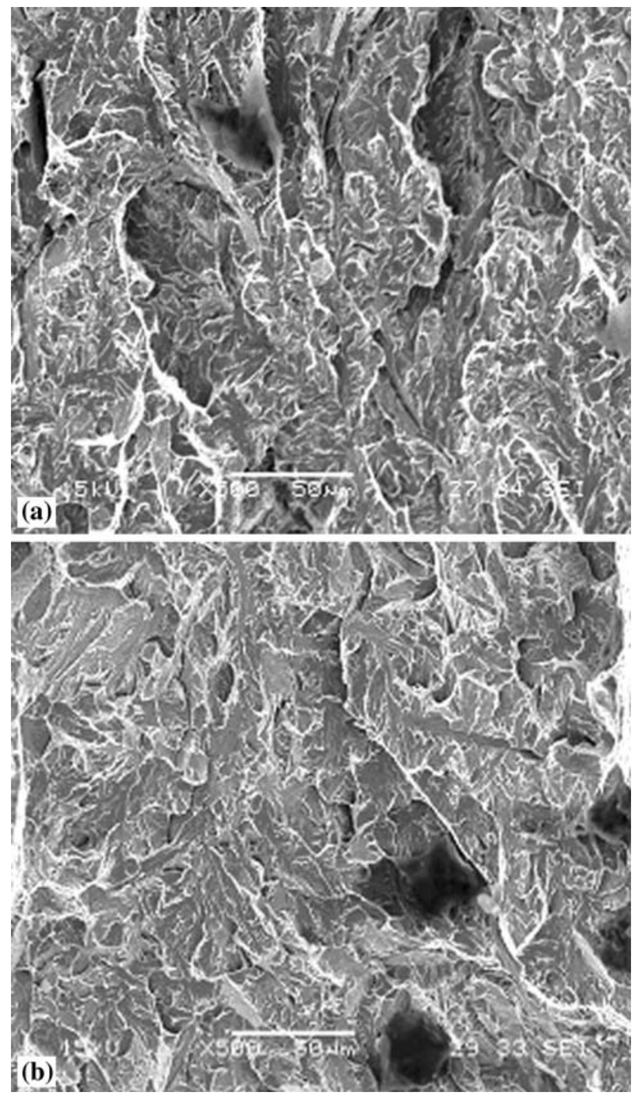

Fig. 8 SEM micrographs of fracture surface of CVN specimen with 0.5 wt.% Si, (a) −40 °C, (b) 125 °C

Styrofoam box containing dry ice and denatured alcohol. Duplicate testing was performed at each temperature and average values of impact energies were recorded.

The metallurgical microstructures of all four heats of the tested materials were determined using conventional metallographic techniques and optical microscopy. Beraha's reagent containing 3 g of $K_2S_2O_3$ and 10 g of $Na_2S_2O_3$ in 100 mL of water was used as an etchant for microstructural evaluation. The morphology of failure at the ruptured surfaces of all CVN specimens was analyzed by SEM.

3. Results and Discussion

The optical micrographs of the tested materials are illustrated in Fig. 2-5. An examination of these micrographs revealed austenitic grain boundaries containing finely dispersed tempered martensitic phase, and delta-ferrites. Streaks of martensitic laths oriented in different directions were also visible within the finely dispersed martensitic structures, possibly due to the positioning of metallographic mounts that were different from the rolling direction. The room temperature tensile properties of the heat-treated materials including the yield strength (YS), ultimate tensile strength (UTS), percent elongation (%El), and percent reduction in area (%RA) are given in Table 2. No significant variations in the magnitude of YS, UTS, and %El were seen due to the addition of different Si content. However, the magnitude of %RA was substantially enhanced in the heat containing 1.9 wt.% Si. The improved ductility could be attributed to the softening of this steel due to the presence of higher Si content that may also reduce the hardenability of the T91 grade steels.

As indicated earlier, the purpose of this investigation was to determine the susceptibility of T91 grade steels to rupture under impact loading as a function of Si content. This type of testing can simulate unusually high strain rates during plastic deformation. The two important parameters, evaluated by this testing, were the energy absorbed (ft-lbs) in fracturing the CVN specimens and DBTT. The variation of average impact energy as a function of testing temperature is given in Table 3 for materials containing four levels of Si. The plots of average impact energy versus temperature for steels containing different levels of Si are illustrated in Fig. 6. These data clearly indicate that the energies absorbed in fracturing the CVN specimens were substantially lower at temperatures of

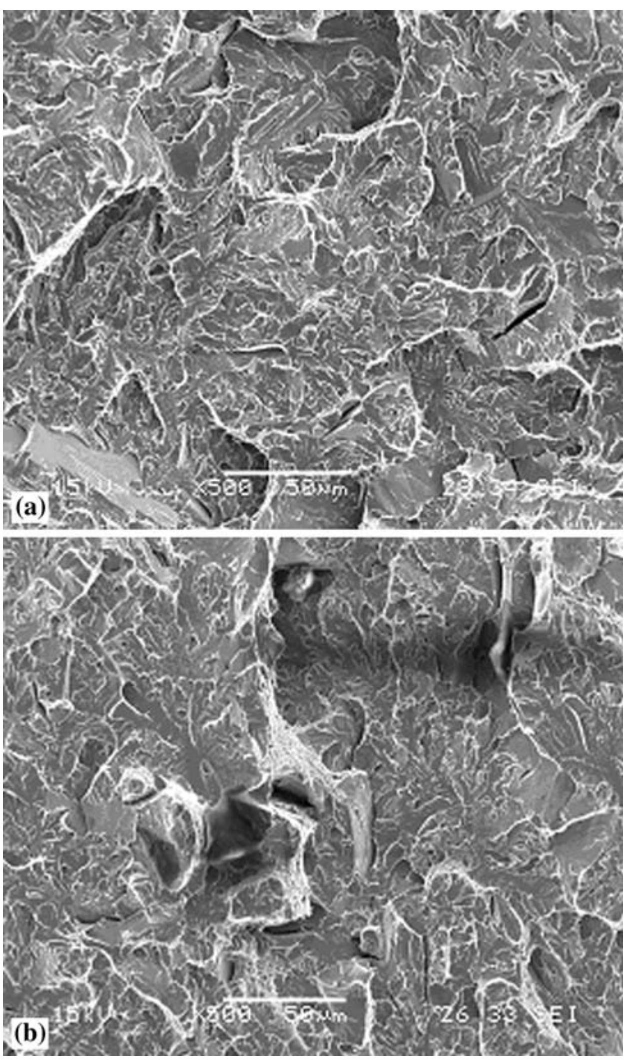

Fig. 9 SEM micrographs of fracture surface of CVN specimen with 1.0 wt.% Si, (a) −40 °C, (b) 125 °C

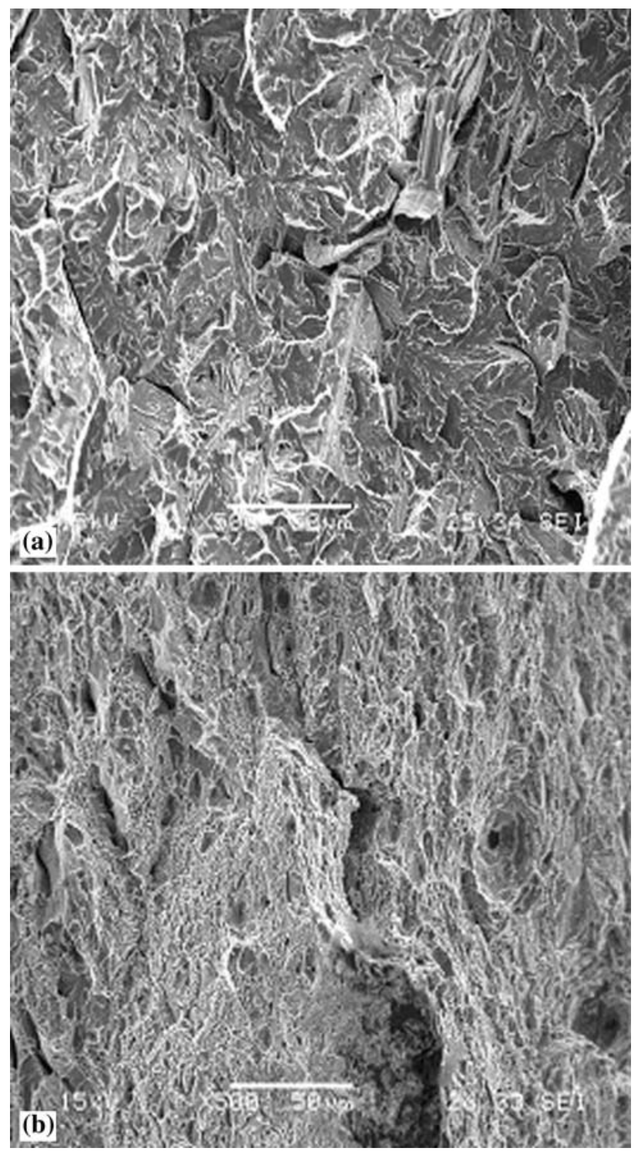

Fig. 10 SEM micrographs of fracture surface of CVN specimen with 1.5 wt.% Si, (a) −40 °C, (b) 125 °C

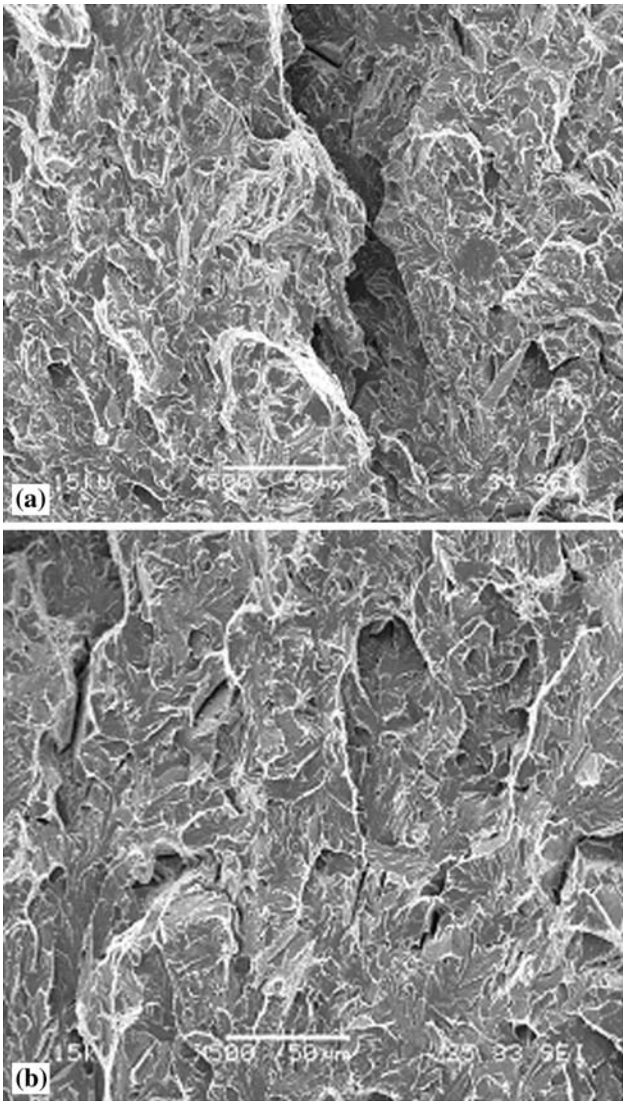

Fig. 11 SEM micrographs of fracture surface of CVN specimen with 1.9 wt.% Si, (a) −40 °C, (b) 125 °C

−40, 25, and 75 °C, as expected, due to reduced ductility at relatively lower temperatures. On the contrary, the impact energy was gradually enhanced with increasing temperature up to 340 °C, followed by the formation of a plateau at 440 °C, irrespective of the Si content. The gradually reduced impact energy with increased Si content at comparable temperatures could also signify reduced ductility, indicating lower hardenability for the tested materials.

The nature of the curves showing the variation of impact energy with temperature, as seen in this investigation, is a general consequence for a majority of engineering metals and alloys indicating the presence of brittle and ductile regions. The portions of this curve showing lower and upper plateaus, respectively, are commonly referred to as the brittle versus ductile region. The linear portion of the curve lying between these two regions signifies a transition from brittle-to-ductile mode of failure. The temperature at which such transition occurs is commonly termed DBTT. The magnitude of DBTT was determined by taking an average value of the impact energy lying between the upper and lower shelf energies of

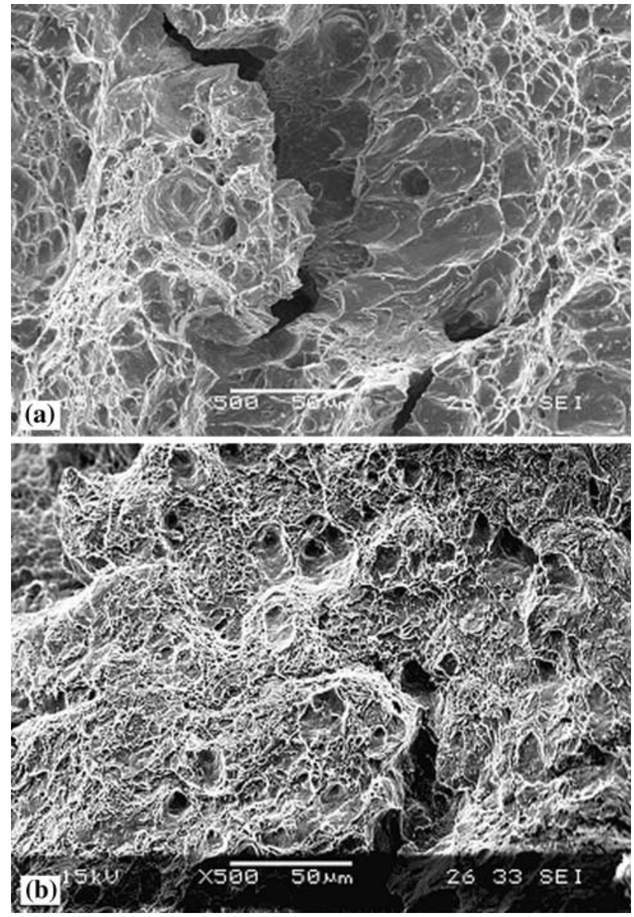

Fig. 12 (a, b) SEM micrographs of fracture surface of CVN specimens tested at 340 °C

steels of varied Si content, and extrapolating this energy value to the temperature axis. The DBTT values corresponding to different levels of Si content are also included in Table 3.

The variation of DBTT with Si content is illustrated in Fig. 7, showing a gradual increase in DBTT with increasing Si content. A higher DBTT value signifies a relatively lower impact resistance showing greater impact energies. Thus, the resultant data clearly suggest that the T91 grade steels with higher Si content would undergo brittle failure more readily than those with lower Si content. Metallurgically speaking, it is preferable for a structural material to possess a DBTT value as low as possible. Thus, these results indicate that the presence of higher Si content in T91 grade steels would be detrimental from the impact resistance point of view.

The SEM micrographs of the fracture surfaces of the CVN specimens tested at −40 and 125 °C are illustrated in Fig. 8-11. An evaluation of these micrographs reveals that all four tested alloys exhibited brittle failures at both temperatures, which were characterized by cleavage and intergranular failure. At an elevated temperature (340 °C), the steel containing 1.9 wt.% Si exhibited combined ductile (dimples) and brittle (intergranular cracking) failures, as shown in Fig. 12(a). On the other hand, the morphology of failure of the steels containing lower Si levels (0.5 wt.%) was ductile, showing dimpled microstructures (Fig. 12b).

4. Summary and Conclusion

The role of Si content on the impact resistance of T91 grade steels has been investigated at temperatures ranging from −40 to 440 °C using CVN specimens. The fracture morphology of the tested specimens has also been determined by SEM. The significant results and the key conclusions derived from this investigation are summarized below.

- As expected, the optical micrographs revealed fine tempered martensites within prior austenitic grains. Delta-ferrites were also seen in these micrographs due to the presence of high chromium content.
- Classical impact energy versus temperature curves resulted, showing upper and lower shelf energies. Lower impact energies and higher DBTT values were observed with the steels containing 1.5 and 1.9 wt.% Si, suggesting a detrimental effect of Si content above 1.0 wt.% for application in the transmutation process.
- All specimens exhibited a combination of intergranular cracking and cleavage failure at lower temperatures irrespective of the Si content. However, the steels containing higher Si levels showed both ductile and brittle failures at elevated temperatures.

Acknowledgment

The financial assistance of the United States Department of Energy, under grant number DE-FC07-06 ID14781, is thankfully acknowledged.

References

1. G. Gupta, Z. Jiao, A.N. Ham, J.T. Busby, and G.S. Was, Microstructural Evolution of Proton Irradiated T91, *J. Nucl. Mater.*, 2006, **351**, p 162–173
2. X. Zia, et al., Microstructure in Martensitic Steels T91 and F82H After Irradiation in SINQ Target-3, *J. Nucl. Mater.*, 2003, **318**, p 207–214
3. Y. Dai, et al., Mechanical Properties of Modified 9Cr-1Mo (T91) Irradiated at ≤ 300°C in SINQ Target-3, *J. Nucl. Mater.*, 2003, **318**, p 192–199
4. Y. Dai, *Proceedings of ICANS-XIII and ESS-PM4*, October 1995, p 604
5. R.L. Klueh, *Proceedings of 1st International Workshop on Spallation Materials Technology*, Oak Ridge, April 1996, p 3–19
6. A.K. Roy and M.K. Hossain, Cracking of Martensitic Alloy EP-823 Under Controlled Potential, *J. Mater. Eng. Perform.*, 2006, **15**, p 336–344
7. A.K. Roy, M.K. Hossain, R. Prabhakaran, and S. Sama, Environment-Assisted Cracking of Structural Materials Under Different Loading Conditions, *Corrosion*, 2005, **61**, p 364–370
8. ASTM Designation E 8-2004, Standard Test Methods for Tensile Testing of Metallic Materials, American Society for Testing and Materials (ASTM) International
9. ASTM Designation E 23-2005, Standard Test Methods for Notched Bar Impact Testing of Metallic Materials, American Society for Testing and Materials (ASTM) International